2010 American Control Conference
Marriott Waterfront, Baltimore, MD, USA
June 30-July 02, 2010

Experimental evaluation of robust-control-relevance: A confrontation with a next-generation wafer stage

Robbert van Herpen, Tom Oomen, Marc van de Wal, Okko Bosgra

Abstract— **Control-relevance is a paradigm that interconnects identification with successive model-based control design. Hereby, the current controller, used to conduct identification experiments, is an important factor to success in the design of a new, improved controller. The aim of this paper is to investigate the role of the experimental controller in robust-control-relevant modeling. Such a study is sensible only when unnecessary conservatism is prevented in the construction of perturbed model sets. Hereto, this paper establishes a model uncertainty description that transparently connects to the imposed robust performance criterion. By confronting the developed approach with a next-generation industrial wafer stage, the important role of the experimental controller during modeling for robust control is clarified indeed. It turns out that only after an increase of performance in successive control design iterations, construction of higher order model sets becomes both feasible and significant. As such, in pursuit of performance optimization up to fundamental limits, the experimental controller ensures a gradual extrapolation of the current experimental conditions.**

I. INTRODUCTION

Scientific modeling entails the creation of a mathematical abstraction of reality. Since any model inherently is approximative in nature, it is futile to strive after a full complexity description of true systems, [8]. This specifically applies to modeling of next-generation high-precision positioning systems, see, *e.g.*, [20], which rely on ever more lightweight, mechanical stages. Typically, such stages exhibit intrinsically multivariable resonance behavior, related to flexible dynamics of the system. To enable the compensation of flexibilities, commonly used rigid-body models have to be extended with an accurate description of flexible phenomena, as is also discussed in, *e.g.*, [1]. However, identification of highly complex models is numerically infeasible, [3]. Consequently, modeling effort needs to be directed towards an accurate characterization of those phenomena, of which compensation is particularly important for high-performance system motion.

First attempts to a symbiosis of system identification and controller synthesis have resulted in the origin of iterative performance optimization schemes, [16]. However, as these schemes fully rely on nominal models of true system behavior, convergence may be hampered by model imperfections, [9]. The need to incorporate robustness as an integral part of the iterative design schemes is acknowledged in [10], [21]. Robustness in the ν-gap metric is introduced in [19]. A further extension towards the dual-Youla parametrization for the description of uncertainty [5] is proposed in [4]. This enables robust control design, [22], which provides a guaranteed performance certificate with a designed controller. Herewith, a monotonous decrease of worst-case performance in successive iterations can be enforced.

Although appropriate experimental conditions have been well acknowledged as an important prerequisite for profitable mutual interdependence of system identification and robust control, see [8] for an overview, the role of the experimental controller has largely remained unstudied. Yet, this controller is a crucial connecting factor between both design steps. In fact, it inevitably forms an integral part of any performance cost function dictating control-relevance, [18]. Particularly, in line with the philosophy in [17], the *current* experimental controller determines the input regime under which the true plant under study is operated. As such, it has dominant influence on the construction of a 'control-relevant' model set, intended to serve as a basis for the synthesis of a robust controller with *improved* performance.

The main contribution of this paper is an investigation into the role of the experimental controller in the synthesis of robust-control-relevant model sets. To enable a sensible analysis, it is key to prevent nullification of control-relevant phenomena, accurately described by a nominal model, in a rigorous uncertainty set. Thereto, a novel coprime-factor coordinate framework is introduced, that transparently connects the classification of model uncertainty to the imposed robust performance criterion. Thus, tight model sets are constructed, tailored to high-performance robust control.

The interplay between the experimental controller and robust-control-relevant identification is evaluated by a confrontation of the approach with a next-generation industrial wafer stage. In particular, the effect of a variation of the nominal plant model-order is studied in this paper, both for a controller with a significantly smaller bandwidth than the desired specification, and a controller that already meets the intended design specifications much closer. To facilitate a fair comparison, the performance goal is fixed, although in practice, gradual adjustment of this goal may be desirable in pursuit of ultimate performance, see also [7].

The paper is organized as follows. First of all, Section II introduces a joint identification and robust control design scheme. Hereafter, Section III discusses identification of a control-relevant coprime factor plant model. Section IV shows a transparant extension towards the dual-Youla uncertainty configuration. Subsequently, Section V derives amplitude bounds on the resulting plant set. Having introduced the key ingredients of robust-control-relevant identification, Section VI analyses the effect of nominal model order variations with a low-performance controller in the loop. A similar analysis is conducted in Section VII for increased performance of the experimental controller, followed by a discussion in Section VIII.

Robbert van Herpen, Tom Oomen and Okko Bosgra are with the Faculty of Mechanical Engineering, Control Systems Technology group, Eindhoven University of Technology, The Netherlands (corresponding author: R.M.A.v.Herpen@tue.nl).

Marc van de Wal is with ASML Research Mechatronics, Veldhoven, The Netherlands. The research reported here has been supported by Philips Applied Technologies, Eindhoven, The Netherlands.

II. PROBLEM FORMULATION

This section formulates the robust-control-relevant identification problem, built on a uniform measure of performance.

Definition 1. The control performance cost J of a given closed-loop configuration is defined as follows:

$$J(P,C) = \|W\,T(P,C)\,V\|_\infty\,. \tag{1}$$

Here, the closed-loop transfer function matrix $T(P,C)$ governs the mapping from the exogenous inputs $[r_2 \quad r_1]^T$ to the exogenous outputs $[y \quad u]^T$ of the standard feedback configuration depicted in Fig. 1:

$$T(P,C) := \begin{bmatrix} P \\ I \end{bmatrix} (I+CP)^{-1} \begin{bmatrix} C & I \end{bmatrix}. \tag{2}$$

Furthermore, $W = \mathrm{diag}(W_y, W_u)$ and $V = \mathrm{diag}(V_2, V_1)$ are bistable weighting filters. This requirement is nonrestrictive, since the weighting filters can be absorbed in the plant using well-established loop-shaping design methods, [11].

Goal 2. Control design aims at obtaining the controller:

$$C_{opt} = \arg\min_C J(P_o, C), \tag{3}$$

where P_o denotes the true system.

Since P_o is unknown, a model set $\mathcal{P}$ is constructed in such a way, that it accurately reflects true plant dynamics, *i.e.*, $P_o \in \mathcal{P}$, *cf.* Section IV-B. Worst-case performance of a given controller is now associated with this set.

Definition 3. Worst-case performance J_{WC} is defined as:

$$J_{WC}(\mathcal{P}, C) = \sup_{P\in\mathcal{P}} J(P,C). \tag{4}$$

It is immediate that the control performance cost achieved for the true plant satisfies:

$$J(P_o, C) \le J_{WC}(\mathcal{P}, C). \tag{5}$$

This observation forms the essence for a joint identification and robust control design scheme, also employed in [4].

Algorithm 4. The upper bound (5) is tightened monotonously by alternating between identification of a robust-control-relevant model set $\mathcal{P}$ and design of a robust controller C. Specifically, at iteration i the following steps are taken:

1) Construction of the smallest perturbed model set:

$$\mathcal{P}^{<i+1>} = \arg\min_{\mathcal{P}} J_{WC}(\mathcal{P}, C^{<i>}), \tag{6}$$

$$\text{subject to:} \quad P_o \in \mathcal{P}^{<i+1>}.$$

2) Optimization of robust performance by control design:

$$C^{<i+1>} = \arg\min_C J_{WC}(\mathcal{P}^{<i+1>}, C). \tag{7}$$

The forthcoming sections describe how to obtain robust-control-relevant model sets $\mathcal{P}$ in more detail.

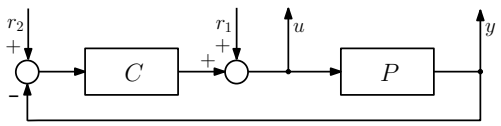

Fig. 1. Standard feedback configuration.

III. PARAMETRIC COPRIME FACTOR FITTING

Control-relevant nominal modeling constitutes an essential basis in the construction of tight model sets for robust control. A justified identification criterion for such model $\hat{P}$ is derived by interrelating *designed* performance cost $J(\hat{P}, C)$ and *achieved* performance cost $J(P_o, C)$, for a given stabilizing controller C, by means of the triangle inequality:

$$J(P_o,C) \le J(\hat{P},C) + \|W\,(T(P_o,C) - T(\hat{P},C))\,V\|_\infty. \tag{8}$$

Clearly, as a prerequisite for successful control design, *performance degradation*, reflected by the rightmost term in (8), should be small. Thus, the following control-relevant nominal identification criterion is derived naturally, [16]:

Proposition 5. Identification of a control-relevant nominal model P is established by solving:

$$P = \arg\min_{\hat{P}} \|W\,(\,T(P_o,C) - T(\hat{P},C)\,)\,V\|_\infty\,. \tag{9}$$

where a highly accurate characterization of closed-loop system behavior $T(P_o, C)$ is available from experiments.

Low-order parametric models are favorable for norm-based control design. To facilitate extension of models with a control-relevant perturbation model, as discussed in Section IV, coprime factor decompositions are established.

Definition 6. The pair $\{N, D\}$ is a right coprime factorization (RCF) of a plant P if: $N, D \in \mathcal{RH}_\infty$, $P = ND^{-1}$, and $\exists\, X, Y \in \mathcal{RH}_\infty$ that satisfy the Bézout identity, [6]:

$$XD + YN = I. \tag{10}$$

In a dual way, a left coprime factorization (LCF) $P = \tilde{D}^{-1}\tilde{N}$ is defined.

Criterion (9) can be transformed into an equivalent control-relevant coprime factor identification criterion.

Proposition 7. Let $\{\tilde{N}_e, \tilde{D}_e\}$ be a LCF of $[CV_2\ V_1]$ with co-inner numerator, [14], where $\tilde{N}_e = [\tilde{N}_{e,2}\ \tilde{N}_{e,1}]$. The control-relevant parametric identification criterion (9) is equivalently solved by the following 2-block criterion:

$$\{N,D\} = \arg\min_{\{\hat{N},\hat{D}\}} \max_{\omega_\ell\in\Omega_{id}} \bar{\sigma}\left(W\left(\begin{bmatrix} N_o \\ D_o \end{bmatrix} - \begin{bmatrix} \hat{N} \\ \hat{D} \end{bmatrix}\right)\Big|_{\omega=\omega_\ell}\right)$$
$$\text{subject to:} \quad T(\hat{P},C) \in \mathcal{RH}_\infty\,, \tag{11}$$

$$\text{where} \qquad \begin{bmatrix} N_o \\ D_o \end{bmatrix} = T(P_o,C)\,V\,[\tilde{N}_{e,2} \quad \tilde{N}_{e,1}]^H, \tag{12}$$

$$\begin{bmatrix} \hat{N} \\ \hat{D} \end{bmatrix} = \begin{bmatrix} \hat{P} \\ I \end{bmatrix} (\tilde{D}_e + \tilde{N}_{e,2}V_2^{-1}\hat{P})^{-1}\,. \tag{13}$$

Proof: A complete proof, including a proof of coprimeness for $\{N, D\}$, is given in [13]. The main step is to make use of:

$$T(P,C)V = \begin{bmatrix} P \\ I \end{bmatrix} (\tilde{D}_e + \tilde{N}_{e,2}V_2^{-1}P)^{-1}[\tilde{N}_{e,2} \quad \tilde{N}_{e,1}], \tag{14}$$

and exploit that $\bar{\sigma}(XY) = \bar{\sigma}(X)$ for any co-inner matrix Y.

Observe that the $\mathcal{H}_\infty$-norm in (9) is approximated by a lower bound in (11). This is inevitable, since the true plant

coprime factors $\{N_o, D_o\}$ are calculated from the closed-loop frequency response functions (FRFs) in $T(P_o, C)$, which have been determined on a discrete frequency grid Ω_{id}. As a consequence, it is required to verify explicitly that the obtained model $\hat{P}$ is stabilized by the controller. Yet, as shown in [13], stability of the factors $\{N, D\}$, which is a prerequisite for coprimeness, is a sufficient requirement to guarantee $T(\hat{P}, C) \in \mathcal{RH}_\infty$.

IV. CONTROL-RELEVANT CLOSED-LOOP PERTURBATION SET

In this section, the nominal model is extended with a perturbation set to account for unmodeled true plant dynamics. The control-relevant uncertainty structure *par excellence* is provided by the dual-Youla parametrization.

Proposition 8. Let $\hat{P}$ be a model that is known to be stabilized by a feedback controller C. In addition, let $\{\hat{N}, \hat{D}\}$ and $\{N_c, D_c\}$ be any RCF of $\hat{P}$ and C, respectively. The set $\mathcal{P}_{dY}$ of all plants that are stabilized by C is defined by, [6]:

$$\mathcal{P}_{dY}(C) := (\hat{N} + D_c\Delta_u)(\hat{D} - N_c\Delta_u)^{-1},\ \Delta_u \in \mathcal{RH}_\infty. \quad (15)$$

Since previously conducted identification experiments have shown C to be stabilizing on the true plant, it is guaranteed that $P_o \in \mathcal{P}_{dY}$ is achieved for some stable perturbation block Δ_u. On the other hand, the set does not contain models that are not stabilized by C, thus avoiding conservatism in subsequent robust control design steps.

A. Towards transparent incorporation of model uncertainty

The main result of this section is a transparant interconnection of the dual-Youla uncertainty description with the imposed robust performance criterion. The following two lemmas are needed.

Lemma 9. Consider the candidate model set $\mathcal{P}_{dY}(C)$ of all plants stabilized by a known feedback controller C. The corresponding set of weighted, perturbed closed-loop models is given by the upper linear fractional transformation (LFT) $\mathcal{F}_u(\hat{M}, \Delta_u)$, where $\hat{M}$ governs the mapping, [4], [13]:

$$\begin{bmatrix} y_\Delta \\ z \end{bmatrix} = \hat{M} \begin{bmatrix} u_\Delta \\ w \end{bmatrix}, \text{ with:}$$

$$\hat{M} = \left[\begin{array}{c|c} 0 & (\hat{D} + C\hat{N})^{-1}\begin{bmatrix} C & I \end{bmatrix} V \\ \hline \begin{bmatrix} W_y D_c \\ -W_u N_c \end{bmatrix} & W \begin{bmatrix} \hat{P} \\ I \end{bmatrix} (I + C\hat{P})^{-1}\begin{bmatrix} C & I \end{bmatrix} V \end{array}\right]. \quad (16)$$

Proof: Straightforward, by substitution of the dual-Youla perturbed plant set, depicted schematically in Fig. 2, in the feedback loop shown in Fig. 1.

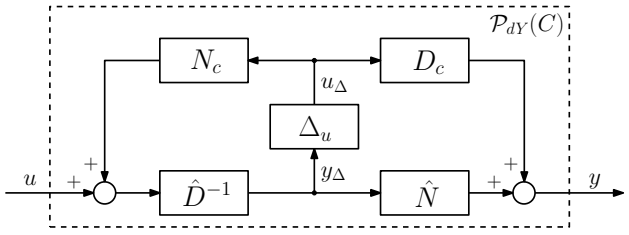

Fig. 2. Dual-Youla perturbed plant set.

Lemma 10. Let U_1 be an inner transfer function matrix, *i.e.*, $U_1^H U_1 = I$, and U_2 be a co-inner transfer function matrix, *i.e.*, $U_2 U_2^H = I$. The $\mathcal{H}_\infty$-norm of a transfer function G is invariant with respect to transformations with such matrices:

$$\|U_1 G U_2\|_\infty = \|G\|_\infty. \quad (17)$$

Proof: see, *e.g.*, [22, Section 13.6].

Lemma 9 and Lemma 10 are exploited to derive the main result of this section:

Proposition 11. [14] The worst-case performance cost J_{WC} satisfies the following upper bound:

$$J_{WC} = \|\mathcal{F}_u(\hat{M}, \Delta_u)\|_\infty \le \|\hat{M}_{22}\|_\infty + \|\Delta_u\|_\infty. \quad (18)$$

Proof: Using the LFT definition, see, *e.g.*, [6], here gives:

$$\begin{aligned} \mathcal{F}_u(\hat{M}, \Delta_u) :&= \hat{M}_{22} + \hat{M}_{21}\Delta_u(I - \hat{M}_{11}\Delta_u)^{-1}\hat{M}_{12} \\ &= \hat{M}_{22} + \hat{M}_{21}\Delta_u\hat{M}_{12}, \end{aligned} \quad (19)$$

since $\hat{M}_{11} = 0$, *cf.* Lemma 9. By virtue of the particular coprime factorization of $\begin{bmatrix} CV_2 & V_1 \end{bmatrix}$ in Proposition 7:

$$\begin{aligned} \hat{M}_{12} &= \hat{D}^{-1}(I + C\hat{P})^{-1}\tilde{D}_e^{-1}\tilde{N}_e \\ &= \hat{D}^{-1}(\tilde{D}_e + \tilde{N}_{e,2}V_2^{-1}\hat{P})^{-1}\tilde{N}_e = \begin{bmatrix} \tilde{N}_{e,2} & \tilde{N}_{e,1} \end{bmatrix}, \end{aligned} \quad (20)$$

where the latter equality follows from (13). Hence, $\hat{M}_{12}$ is co-inner by construction. Moreover, $\hat{M}_{21}$ is rendered inner by selecting a (W_u, W_y)-normalized factorization of C, [14]. Finally, by applying the triangle inequality to (19) and making use of Lemma 10, the proof is completed.

The importance of Proposition 11 lies in the fact that the size of the admissible set of perturbations Δ_u directly affects the worst-case performance cost. Different coprime factor realizations yield a non-transparent interpretation of model uncertainty, since $\hat{M}_{21}$ and $\hat{M}_{12}$ deform the contribution of perturbations to the worst-case performance cost in that case.

B. Establishing tight model sets for robust control

Having developed a control-relevant perturbation structure, it remains to determine a justified bound γ on the set of admissible perturbations $\mathbf{\Delta_u}$ exploited in robust control design:

$$\mathbf{\Delta_u} := \{\Delta_u \in \mathcal{RH}_\infty,\ \|\Delta_u\|_\infty \le \gamma\}. \quad (21)$$

By virtue of Proposition 11, minimization of γ provides maximum room for performance optimization. On the other hand, however, the resulting plant set $\mathcal{P}_{dY}$ in (15) should be large enough to ensure that $P_o \in \mathcal{P}$.

In [12], a deterministic model validation procedure is proposed that facilitates tight perturbation modeling for robust control. The approach employs the setup in Fig. 3, wherein the true feedback loop is denoted by M_o. Next to the response to manipulated inputs w, the measured outputs z_m exhibit influences of external disturbances that affect the true system. Inevitably, the single nominal closed-loop model $\hat{M}_{22}$ is incapable of fully explaining observed behavior. By (i) extension towards the perturbed closed-loop model set $\mathcal{F}_u(\hat{M}, \Delta_u)$, and (ii) addition of a disturbance model v, the observed model-reality mismatch can be explained, *i.e.*, $\varepsilon = 0$, can be achieved.

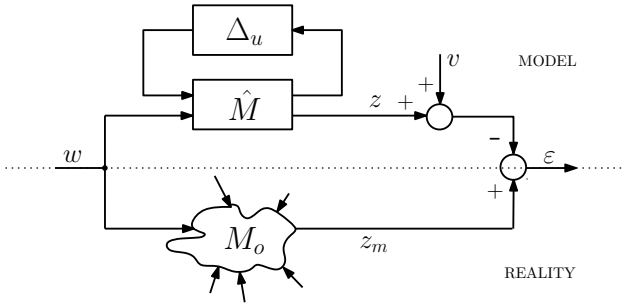

Fig. 3. Model validation setup.

A disturbance model is part of any realistic validation procedure, where it serves to avoid conservatism in uncertainty modeling. Although disturbance phenomena contribute to the observed model-reality mismatch, they clearly should not be classified as input-output behavior of the true system. Periodic validation experiments form a key instrument to discriminate disturbance phenomena from unmodeled true system dynamics, which, in contrast to disturbances, manifest themselves repeatedly in the observed model-reality mismatch. This fundamental observation provides a basis to exclude disturbance phenomena from the uncertainty discription, yielding a least conservative bound γ on the admissible perturbation set (21), see [12] for details.

V. MAGNITUDE BOUNDS ON THE PLANT SET

This section derives bounds on the obtained robust-control-relevant plant set for the SISO case, enabling an intuitive visual interpretation in the sequel. The dual-Youla parametrization (15) is a bilinear transformation, which can be decomposed into four elementary mappings, [2]:

$$w = \frac{az+b}{cz+d} = \frac{bc-ad}{c^2} \cdot \frac{1}{z+\frac{d}{c}} + \frac{a}{c}. \qquad (22)$$

Indeed, (15) is obtained by selecting:
$a = D_c\,,\ b = \hat{N}\,,\ c = -N_c\,,\ d = \hat{D}\,,\ z = \Delta_u\,,\ w = \mathcal{P}_{dY}.$

The bilinear transformation is a conformal mapping. That is, circles are mapped onto circles, characterized as follows.

Lemma 12. Consider a complex circle z, with radius γ centered around the origin. After bilinear transformation, a new circle results with center C_{bt} and radius R_{bt}, where:

$$C_{bt} := \frac{(d/c)^*}{|d/c|^2 - \gamma^2} \cdot \frac{bc-ad}{c^2} + \frac{a}{c}, \qquad (23)$$

$$R_{bt} := \frac{\gamma}{\big|\,|d/c|^2 - \gamma^2\,\big|} \cdot \left|\frac{bc-ad}{c^2}\right|. \qquad (24)$$

Proof: Follows directly from (22), see also, *e.g.*, [5].

Observe that the center of the circle z (which represents the nominal plant $\hat{P}$) does not map onto the center of the circle w (*i.e.*, the set $\mathcal{P}_{dY}$). Using Lemma 12, the following bounds are derived for the plant set $w \simeq \mathcal{P}_{dY}$:

Proposition 13. The lower bound M_l and upper bound M_u on the magnitude of plants $P \in \mathcal{P}_{dY}$ are given by:

$$M_l = \begin{cases} 0\ , \text{ if } \quad R_{bt} > |C_{bt}| \\ \qquad\quad \text{and } \ |\gamma| \le \left|\frac{d}{c}\right|\ , \\ \left|\, C_{bt} - \left(\frac{C_{bt}}{|C_{bt}|} \cdot R_{bt}\right)\right|, \text{ otherwise .} \end{cases} \qquad (25)$$

$$M_u = \begin{cases} \infty\ , \text{ if } \ |r| > \left|\frac{d}{c}\right|\ , \\ \left|\, C_{bt} + \left(\frac{C_{bt}}{|C_{bt}|} \cdot R_{bt}\right)\right|, \text{ otherwise .} \end{cases} \qquad (26)$$

The lower bound (25) equals zero when the transformed circle w encloses the origin. On the other hand, the upper bound (26) is infinite when Δ_u that renders (15) singular is admissible. In the latter case, the interior of the circle in w maps onto the exterior of the resulting circle in z.

VI. EVALUATING CONTROL-RELEVANCE – A LOW-PERFORMING CONTROL LOOP

Having connected identification and robust control in a transparant manner, the preconditions for a sensible study into the robust-control-relevance paradigm have been provided. The remainder of this paper considers a confrontation of the described tight modeling methodology, tailored towards high-performance robust control, with a next-generation industrial wafer stage. Due to an outstanding mechatronic design, this machine serves as a representative case study, as it shows highly reproducible, dominantly linear behavior up to very high frequencies. Moreover, due to a large freedom in the design of identification experiments, the approximation error involved in the characterization of closed-loop behavior can be made negligibly small. This enables an investigation into the role of the experimental controller in the construction of robust-control-relevant model sets. In particular, both for a controller with significantly smaller bandwidth than the desired specification and for a controller that meets the intended specification much closer, the effect of a variation of the nominal model order in the construction of model sets for robust control is studied.

A. A next-generation industrial wafer stage

The wafer stage used to conduct experiments, developed by Philips Applied Technologies, Eindhoven, is shown in Fig. 4. Such a wafer stage is part of extremely dedicated lithography machines used for integrated-circuit manufacturing on chips, and serves to position chips with respect to the light source. State-of-the-art wafer stages are operated contactless, on the basis of magnetic levitation. Nanometer accuracy position measurement is made available using laser interferometry, for which the mirror block on top of the stage

i	Landing foot	iv	Zerodure mirror block
ii	Forcer coil	v	Boundary rail
iii	End-of-stroke damper	vi	Permanent magnet plate

Fig. 4. Detail photograph of a wafer stage.

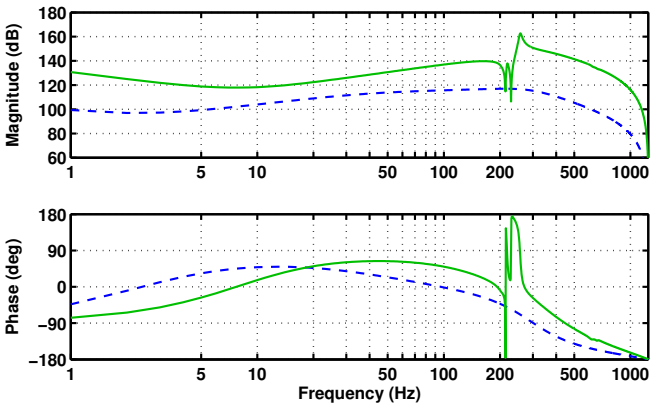

Fig. 5. Initial controller, designed with standard loop-shaping techniques (dashed), and robust controller, synthesized based on the 7th order plant set (solid).

is exploited. To clearly illustrate concepts, one single motion degree of freedom of the wafer stage will be considered only, whereas multivariable results have been obtained as well.

B. Experimental conditions

To characterize closed-loop behavior by means of measurement experiments, a feedback controller needs to be designed first. Conventional approaches, still widely applied in industry, consider multiloop SISO control design. Therefor, although such approach is inadequate due to the intrinsically multivariable, flexible behavior of next-generation wafer stages, conventional manual loop shaping is applied to obtain an initial 10 Hz-bandwidth controller. This controller, depicted in Fig. 5, has integral action and second-order roll-off.

Independent multisine identification and validation experiments, see *e.g.* [15], are conducted on a dense frequency grid to characterize closed-loop behavior. Model validation exploits the complete excitation grid

$$\Omega_{val} = 2\pi[1, 2, \ldots, 1250] \text{ rad/s}, \tag{27}$$

to ensure an accurate representation of true plant dynamics by the constructed robust-control-relevant model set. However, for nominal identification, the following subset is selected:

$$\Omega_{id} = 2\pi[1, 2, \ldots, 890] \text{ rad/s}. \tag{28}$$

On this grid, all four closed-loop transfer function in (2) can be estimated with such high accuracy, that the experimental conditions can be discounted from the forthcoming analysis on control-relevant modeling.

In pursuit of performance optimization, it is desired to improve the control bandwidth to 50 Hz. For this purpose, appropriate performance weights are incorporated in the loop, [11, Chapter 6], that again have integral action and second-order roll-off. Note that, in view of the imposed design requirement, the currently implemented experimental controller is ill-performing indeed.

C. Robust-control-relevant modeling

The first step in robust-control-relevant modeling is the construction of a nominal coprime factor model as described in Section III. To this end, the parametric $\mathcal{H}_\infty$ identification criterion presented in Proposition 7 is solved using a numerically well-conditioned iterative procedure based on Lawson's algorithm, [13]. Figure 6 shows the obtained 7th order plant model, which accurately reflects rigid body behavior (*i.e.*, a double integrator, or mass-line), two dominant resonances and a sample delay that is present in the system.

Based on the conducted validation experiment, the nominal model is extended with an uncertainty description, as discussed in Section IV-B. The resulting plant set is indicated by the shaded area in Fig. 6, which has been computed using the bounds derived in Section V. Indeed, the model set envelopes true plant behavior successfully. On the other hand, the set is tight around those true system artifacts that are reflected accurately by the control-relevant nominal model, thus providing room for performance improvement by means of robust control.

D. Model order selection

A natural question arising here is whether increasing the order of the nominal plant model would lead to the inclusion of additional resonance phenomena in the description of the plant behavior, and herewith to further tightening of the plant

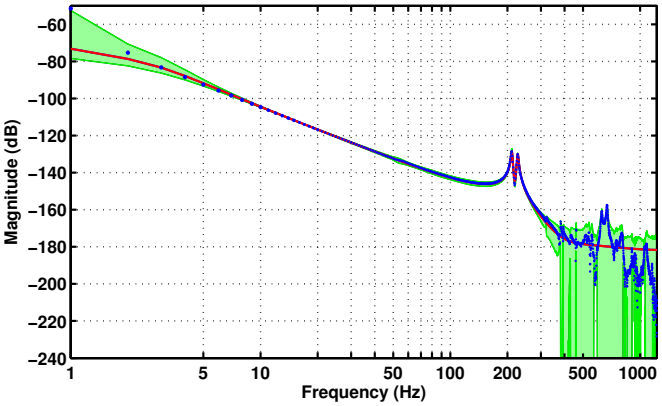

Fig. 6. Bode magnitude plot of the identified transfer function estimate of P_o (dotted), the constructed 7th order coprime factor model $\hat{P}$ (solid), and the candidate plant set $\mathcal{P}_{dY}(C)$ obtained through model validation (green).

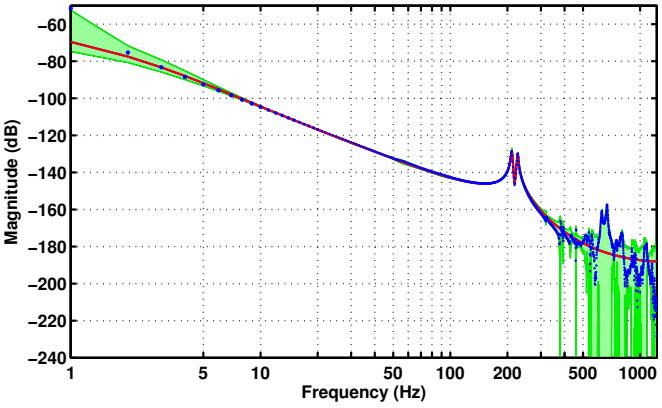

Fig. 7. Identified plant set based on a 9th order model $\hat{P}$.

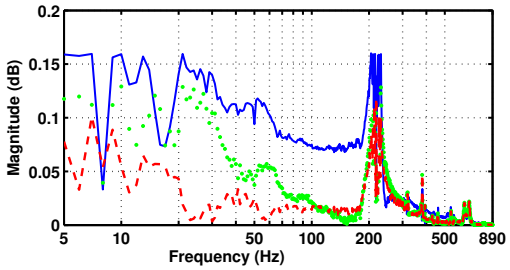

Fig. 8. $\mathcal{H}_\infty$ model mismatch $\|W(T(P_o, C) - T(\hat{P}, C))V\|_\infty$ for the 7th order (solid), 9th order (dotted) and 11th order (dashed) plant model $\hat{P}$.

set at high frequencies. Figure 7 shows the plant set as constructed on the basis of a 9th order nominal model. It turns out that the additional freedom in the nominal model has been used to make small adjustments on the description of the mass-line and the dominant resonances little above 200 Hz, which were included in the 7th order model already. Further increasing the nominal model order to 11 shows the same effect. This is confirmed in Fig. 8, which shows the $\mathcal{H}_\infty$ nominal model-mismatch for varying orders. According to the control-relevant identification criterion, it is most rewarding to match the dominant system resonances even more precisely, next to a more accurate representation of the plant dynamics at the very lowest frequencies.

It is questionable whether the higher order plant models indeed represent true system behavior more appropriately. Recall from (6) that minimization of the worst-case performance cost J_{WC} is the ultimate goal in robust-control-relevant modeling. Hence, to assess the merits of an increased model order, J_{WC} needs to be analyzed. Since model uncertainty has been characterized on the frequency grid Ω_{val} only, the validation procedure described in Section IV-B will provide a nonparametric bound $\gamma(\omega_i)$, $\omega_i \in \Omega_{val}$ on the admissible set of model perturbations (21) only. Clearly, true $\mathcal{H}_\infty$ control design requires an analysis on a continuous frequency grid, which demands for the construction of a bistable parametric overbound on $\gamma(\omega_i)$. For the sake of clarity, the performance cost analysis will be limited to the validation grid instead. On this grid, J_{WC} is computed by means of a skewed-μ analysis, [22], for which the closed-loop model set in Proposition 9 is exploited. Results are presented in Table I.

TABLE I

PERFORMANCE COSTS AS A FUNCTION OF MODEL ORDER.

Nominal model order	5	7	9	11
$\mathcal{H}_\infty$ - mismatch	2.236	0.160	0.129	0.119
$J(\hat{P}, C)$	108.77	111.61	109.67	∞
J_{WC}	111.09	116.55	112.71	∞

As a first comment, it turns out that the 11th order parametric model is built up from unstable factors $\{\hat{N}, \hat{D}\}$. As already mentioned in Section III, this indicates that the obtained model is not stabilized by the experimental controller, in spite of the fact that the closed-loop response of the modeled configuration accurately reflects the identified FRF data. Consequently, especially for the identification of high order models, which is numerically extremely challenging, it is required to integrate additional stability constraints in the coprime factor fitting algorithm of [12]. This is subject to additional research.

From Table I, it is immediate that J_{WC} is dominated by the nominal performance cost $J(\hat{P}, C)$, due to the low performance of the experimental controller. It turns out that the worst-case performance is obtained at 1 Hz for all model orders (actually, steady state turns out to be critical in the true $\mathcal{H}_\infty$ sense). As the full closed-loop transfer function matrix $T(P_o, C)$ is matched at 1 Hz most accurately using the 5th order model, J_{WC} achieves the smallest criterion value for this order. This again raises suspicion about the relevance of the obtained model sets for robust control design. Is accurate representation of behavior at very low frequencies indeed critical to design of a 50 Hz-bandwidth robust controller?

VII. IMPROVED EXPERIMENTAL CONTROLLER

This section discusses the effect of an improvement of experimental controller performance on the obtained robust-control-relevant model sets. In particular, based on the 7th order model in Fig. 6, a robust controller is synthesized. This controller, shown in Fig. 5, explicitly compensates the dominant plant resonances, and achieves a bandwidth of 43 Hz.

After implementation, new experiments are conducted on the wafer stage. This is key to improved modeling, since the plant is now operated with an input regime that is more representative for the intended performance goal, due to improvement of the experimental controller [17]. Consequently, one would expect modeling to be better tailored towards the design of a 50 Hz-bandwidth robust controller.

A. Robust-control-relevant modeling

Again, robust-control-relevant model sets are constructed for varying model orders. The corresponding performance cost indicators are shown in Table II. Here, it is confirmed

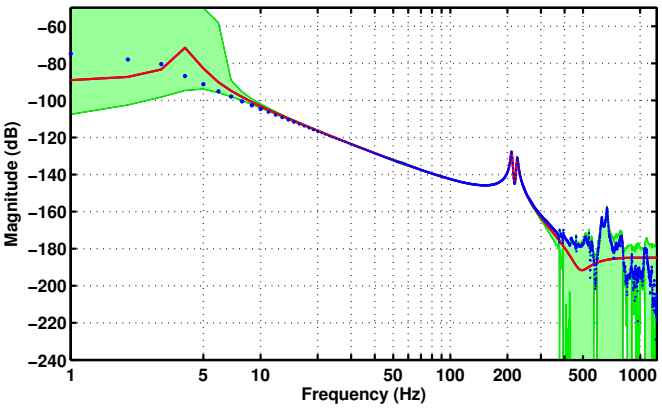

Fig. 9. Identified plant set based on a 7th order model $\hat{P}$.

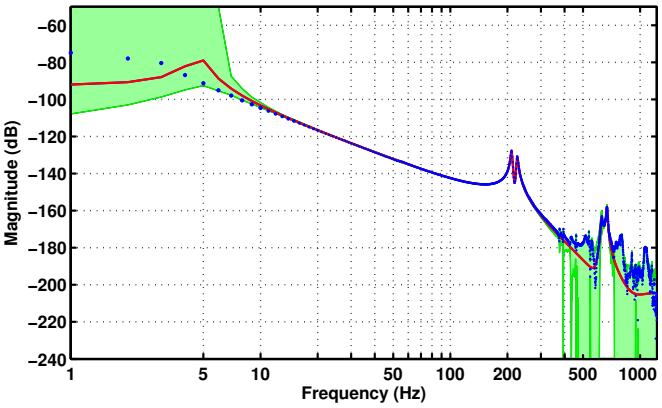

Fig. 10. Identified plant set based on a 11th order model $\hat{P}$.

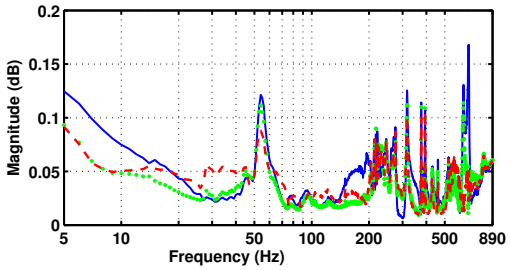

Fig. 11. $\mathcal{H}_\infty$ model mismatch $\|W(T(P_o, C) - T(\hat{P}, C))V\|_\infty$ for the 7th order (solid), 9th order (dotted) and 11th order (dashed) plant model $\hat{P}$.

TABLE II

PERFORMANCE COSTS AS A FUNCTION OF MODEL ORDER.

Nominal model order	5	7	9	11	13
$\mathcal{H}_\infty$ - mismatch	2.214	0.168	0.114	0.106	0.105
$J(\hat{P}, C)$	3.745	3.354	3.310	3.307	3.310
J_{WC}	5.884	3.438	3.431	3.431	3.432

that the designed robust controller leads to significant performance improvement. As hypothesized, this influences the modeling step indeed. Figure 9 depicts the 7th order plant set. A shift of modeling emphasis towards higher frequencies can already be perceived by comparing with Fig. 6. Increasing the order of the nominal model to 11 now leads to an accurate description of the resonance pair around 600 Hz in the nominal model. As a consequence, the plant set is tightened around this frequency, as is clearly observed in Fig. 10. Moreover, the $\mathcal{H}_\infty$ model mismatch clearly improves due to accurate modeling of additional system artefacts, as observed in Fig. 11. Further increasing the order of the nominal model does not lead to modeling of additional resonances, though, and may even carry the risk of overmodeling. As a final comment, although additional resonances have been modeled with high accuracy, an update of the performance weights is required to truly improve robust control performance in a new control design cycle.

VIII. DISCUSSION

In this paper, it is revealed that the experimental controller plays a crucial role in the connection of identification and robust control using the control-relevance paradigm. To enable a sensible study into robust-control-relevance, it is required to prevent the introduction of unnecessary conservatism in the construction of perturbed model sets. Hereto, a transparant connection between the classification of model uncertainty and the imposed robust performance criterion is established in this paper. This leads to the construction of tight model sets, that are directly tailored to high-performance robust control design. Subsequently, the developed approach has been confronted with a next-generation wafer stage. Robust-control-relevant model sets are constructed, both for a controller with a significantly smaller bandwidth than the desired specification as well as a controller that already meets the intended design specifications much closer.

When the performance of the experimental controller is slight in view of the specified control goal, modeling effort is focussed towards an accurate characterization of low-frequent system behavior. As control performance gradually improves in subsequent robust control design steps, higher order model sets can be constructed successfully, in which more and more of the flexible system behavior is described accurately. Instead of demanding robustness with respect to flexibility, explicit compensation of resonance phenomena then becomes feasible, thus leading to increased performance. In conclusion, the experimental controller ensures a gradual extrapolation of the current experimental conditions, to facilitate iterative optimization of robust performance. Eventually, when the specified performance goal is approached, the model set will become tight around those resonance phenomena that would be compensated for when performance requirements would be further increased by the designer. As next-generation wafer stages show deterministic behavior that can be identified up to very high frequencies with large accuracy, this truly enables the pursuit of performance improvement up to fundamental limitations.

This paper confirms the important role of the experimental controller in robust-control-relevant identification, but also gives rise to a further study into the phenomenon of model order selection in a control-relevance setting. It is expected that the worst-case performance cost provides a means for the selection of the smallest nominal model order that still allows for the explanation of control-relevant phenomena. Indeed, Section VII confirms that worst-case performance decreases as more and more control-relevant system artifacts are described accurately in the nominal model. A more detailed analysis is the topic of current research.

REFERENCES

[1] G. J. Balas and J. C. Doyle. Control of lightly damped, flexible modes in the controller crossover region. *AIAA Journal of Guidance, Dynamics and Control*, 17(2):370–377, 1994.

[2] J. W. Brown and R. V. Churchill. *Complex Variables and Applications*. McGraw-Hill, New York, NY, USA, 1996.

[3] A. Bultheel, M. Van Barel, Y. Rolain, and R. Pintelon. Numerically robust transfer function modeling from noisy frequency domain data. *IEEE Transactions on Automatic Control*, 50(11):1835–1839, 2005.

[4] R. A. de Callafon and P. M. J. Van den Hof. Suboptimal feedback control by a scheme of iterative identification and control design. *Mathematical Modeling of Systems*, 3(1):77–101, 1997.

[5] S. G. Douma and P. M. Van den Hof. Relations between uncertainty structures in identification for robust control. *Automatica*, 41(3):439–457, 2005.

[6] B. Francis. A course in $\mathcal{H}_\infty$ control theory. *Lecture Notes in Control and Information Sciences, Springer-Verlag, Berlin*, vol. 88, 1987.

[7] M. Graham and R. de Callafon. Performance weight adjustment for iterative cautious control design. *Proc. European Control Conference, Kos, Greece*, pages 217–222, 2007.

[8] H. Hjalmarsson. From experiment design to closed-loop control. *Automatica*, 41(3):393–438, 2005.

[9] H. Hjalmarsson, S. Gunnarsson, and M. Gevers. Optimality and sub-optimality of iterative identification and control design schemes. In *Proc. American Control Conference, Seattle, WA, USA*, 1995.

[10] W. S. Lee, B. D. O. Anderson, R. L. Kosut, and I. M. Y. Mareels. A new approach to adaptive robust control. *International Journal of Adaptive Control and Signal Processing*, 7(3):183–211, 1993.

[11] D. McFarlane and K. Glover. Robust controller design using normalized coprime factor plant descriptions. *Lecture Notes in Control and Information Sciences*, 138, 1990.

[12] T. Oomen and O. Bosgra. Estimating disturbances and model uncertainty in model validation for robust control. In *Proc. 47th IEEE Conference on Decision and Control, Cancún, Mexico*, pages 5513–5518, 2008.

[13] T. Oomen and O. Bosgra. Robust-control-relevant coprime factor identification: A numerically reliable frequency domain approach. In *Proc. American Control Conference, Seattle, WA, USA*, pages 625–631, 2008.

[14] T. Oomen, R. van Herpen, and O. Bosgra. Robust-control-relevant coprime factor identification with application to model validation of a wafer stage. In *Proc. 15th IFAC Symposium on System Identification, St. Malo, France*, pages 1044–1049, 2009.

[15] R. Pintelon and J. Schoukens. *System Identification: A Frequency Domain Approach*. IEEE Press, New York, NY, USA, 2001.

[16] R. J. P. Schrama. Accurate identification for control: The necessity of an iterative scheme. *IEEE Transactions on Automatic Control*, 37(7):991 – 994, 1992.

[17] R. E. Skelton. Model error concepts in control design. *International Journal of Control*, 49(5):1725–1753, 1989.

[18] P. Van den Hof and R. Schrama. Identification and control – closed-loop issues. *Automatica*, 31(12):1751–1770, 1995.

[19] G. Vinnicombe. Frequency domain uncertainty and the graph topology. *IEEE Transactions on Automatic Control*, 38(9):1371–1383, 1993.

[20] M. van de Wal, G. van Baars, F. Sperling, and O. Bosgra. Multivariable $\mathcal{H}_\infty/\mu$ feedback control design for high-precision wafer stage motion. *Control Engineering Practice*, 10(7):739–755, 2002.

[21] Z. Zang, R. R. Bitmead, and M. Gevers. Iterative weighted least-squares identification and weighted LQG control design. *Automatica*, 31(11):1577–1594, 1995.

[22] K. Zhou, J. C. Doyle, and K. Glover. *Robust and Optimal Control*. Prentice Hall, Upper Saddle River, NJ, USA, 1996.